giving

$$\cos\beta = (1+f-(1+2f)^r)/f. \tag{38}$$

As is shown in Figure 9b all the possible positions of $\mathbf{k}'$ are the generators of a cone, about $\mathbf{k}$, of semi-angle β. If an arbitrary line is drawn on the base of this cone through $\mathbf{k}$ then the end point of $\mathbf{k}'$ that lies on the circular edge is in a position designated by an azimuthal angle ϕ for which $p(\phi)=1$. The relationship of a uniformly distributed random number r to ϕ is $r=\phi/2\pi$.

The post-scattering coordinates (k'_ρ, k'_z) are

$$k'_\rho = |\mathbf{k}'| \sin\gamma, \tag{39a}$$

$$k'_z = |\mathbf{k}'| \cos\gamma, \tag{39b}$$

where γ is the angle between $\mathbf{k}'$ and $\mathbf{F}$ and γ is related to β and ϕ. The latter arises from the vector relationship, shown in Figure 9c,

$$(\mathbf{k}'\times\mathbf{k})\cdot(\mathbf{k}\times\mathbf{F}) = (\mathbf{k}'\cdot\mathbf{k})(\mathbf{k}\cdot\mathbf{F}) - (\mathbf{k}'\cdot\mathbf{F})(\mathbf{k}\cdot\mathbf{k}) \tag{40}$$

This gives immediately

$$-\sin\beta\sin\psi\cos\phi = \cos\beta\cos\psi - \cos\gamma, \tag{41}$$

where ψ is the angle between $\mathbf{k}$, and $\mathbf{F}$. ϕ is the uniformly distributed random angle discussed above. Hence positive and negative values of $\cos\phi$ are equally possible. At the end of a flight the electron position is k_z and its energy is E so that $|\mathbf{k}| = (2m^*E)^{\frac{1}{2}}/\hbar$ and $\cos\psi = k_z/|\mathbf{k}|$.

5.2 Mean velocity and mean energy

The time spent by an electron in each part of $\mathbf{k}$-space is proportional to the electron distribution function and, in principle, this is computed and used to calculate useful mean values, such as the mean electron velocity and the mean electron energy. Indeed, since the Monte Carlo calculation described here is equivalent to an exact solution of the Boltzmann equation for a non-degenerate electron gas, it would seem that the accumulation of the visiting time of an electron in each element of $\mathbf{k}$-space is the primary computing objective.

This procedure, however, would require the establishment of a $\mathbf{k}$-space histogram with quite a fine mesh in order to obtain accurate answers. Fortunately, it is not necessary to do this, although such a histogram, with a reasonable mesh, will be calculated for qualitative purposes. The mean values of velocity and energy can be accumulated directly by monitoring each electron flight and then taking an average over all flights.

For the electron velocity this procedure is understood as follows. The

velocity of an electron is

$$\mathbf{v}=\frac{1}{\hbar}\nabla_{\mathbf{k}}E(\mathbf{k})=\frac{\hbar\mathbf{k}}{m^*} \tag{42}$$

and, since the motion in **k**-space along the k_z-axis is uniform, $p(k_z)=1$. This means that, for all flights from starting positions k_{zi} to final positions k_{zf}, the mean drift velocity is defined as

$$v=\frac{\dfrac{\hbar}{m^*}\sum\int_{k_{zi}}^{k_{zf}}k_z\,\mathrm{d}k_z}{\sum\int_{k_{zi}}^{k_{zf}}\mathrm{d}k_z}=\frac{\sum\int_{k_{zi}}^{k_{zf}}\dfrac{1}{\hbar}\dfrac{\partial E}{\partial k_z}\,\mathrm{d}k_z}{\sum\int_{k_{zi}}^{k_{zf}}\mathrm{d}k_z}=\frac{\sum(E_f-E_i)}{\hbar D}, \tag{43}$$

where the summation is over all electron flights that occur during the simulation and $1/D$ is the distribution function per unit length of the **k**-space flight. The same reasoning leads to a mean energy E being defined as

$$E=\frac{\hbar^2}{2m^*}\frac{\sum\int_{k_{zi}}^{k_{zf}}(k_\rho^2+k_z^2)\,\mathrm{d}k_z}{\sum\int_{k_{zi}}^{k_{zf}}\mathrm{d}k_z}. \tag{44}$$

This technique avoids the setting up of a histogram mesh that is fine enough to ensure a convergent result. All that is required is the accumulation of contributions from each flight, thus making the simulation both accurate and very much easier to program.

Naturally v and E are accumulated for each valley and the mean values for the whole valley structure are then calculated by weighting each contribution according to the electron population ratio. The quantity D, when multiplied by $\hbar/eF$, gives the total time spent by the electron in a valley. If T_c is the time spent in the central valley and T_s the time spent in the satellite valleys then $N1=T_c/(T_c+T_s)$ and $N2=T_s/(T_c+T_s)$ give the relative electron population ratios of the valleys. The evaluation of the integrals in equations (43) and (44) leads to the following expressions for v and E:

$$v=\frac{\hbar}{2m^*D}\sum(k_{zf}^2-k_{zi}^2) \tag{45}$$

and

$$E=\frac{\hbar^2}{2m^*D}\sum\left\{k_\rho^2(k_{zf}-k_{zi})+\frac{(k_{zf}^3-k_{zi}^3)}{3}\right\}. \tag{46}$$

6. COMPUTER PROGRAMS

6.1 Description

The optimum use of the programs, listed at the end of this chapter, is in an interactive mode on the type of computer terminal that has a visual display unit (VDU) with a graphics capability. In the interactive mode the program prompts the user to input data or to execute other actions as the calculation proceeds. If only an ordinary terminal is available the program can still be used by omitting the graphics package or suitably editing it to work off-line. This may require the deletion of specific reference to the VDU and feeding in the required data in a modified manner.

The main program is called CARLO and the graph plotting program is called GMONTE. The compiled, loaded, ready to run, binary versions are called *CARLO and *GMONTE. The files that are used are:

FILE	*CONTENTS*
MONTEF:	complete tables of final results
MDATA 1:	electric field values
MDATA 2:	mean velocities
MDATA 3:	mean energies
MDATA 4:	**k**-space histograms
MDATA 5:	input data
GRAPP:	test labels for choice of action

All these files are established as reading, writing, or reading/writing files by the instruction CALL SEARCH (a, 'FILE', b) where a = 1 denotes a file from which information is read, a = 2 denotes a file into which information is written, and a = 3 denotes the reading/writing mode. Here, b is an arbitrary file number. Since files are of variable length two actions are normally used to close them. The first

CALL SEARCH (8, 0, b)

truncates the file, while the second

CALL SEARCH (4, 0, b)

actually closes it. For reading and writing the VDU has device number 1 but reading out of and writing into the files uses b+4.

Subroutines CALL ZREALD (A), CALL ZINTRD (A) are used that halt the program until a piece of data or an instruction is entered or the computer is simply requested to proceed. Actually these are free-format instructions that enable data to be entered in free format into A or, if RETURN is activated treat A as dummy and pass on to the next instruction. CALL PAGE is a little subroutine that clears the VDU screen. RESUME

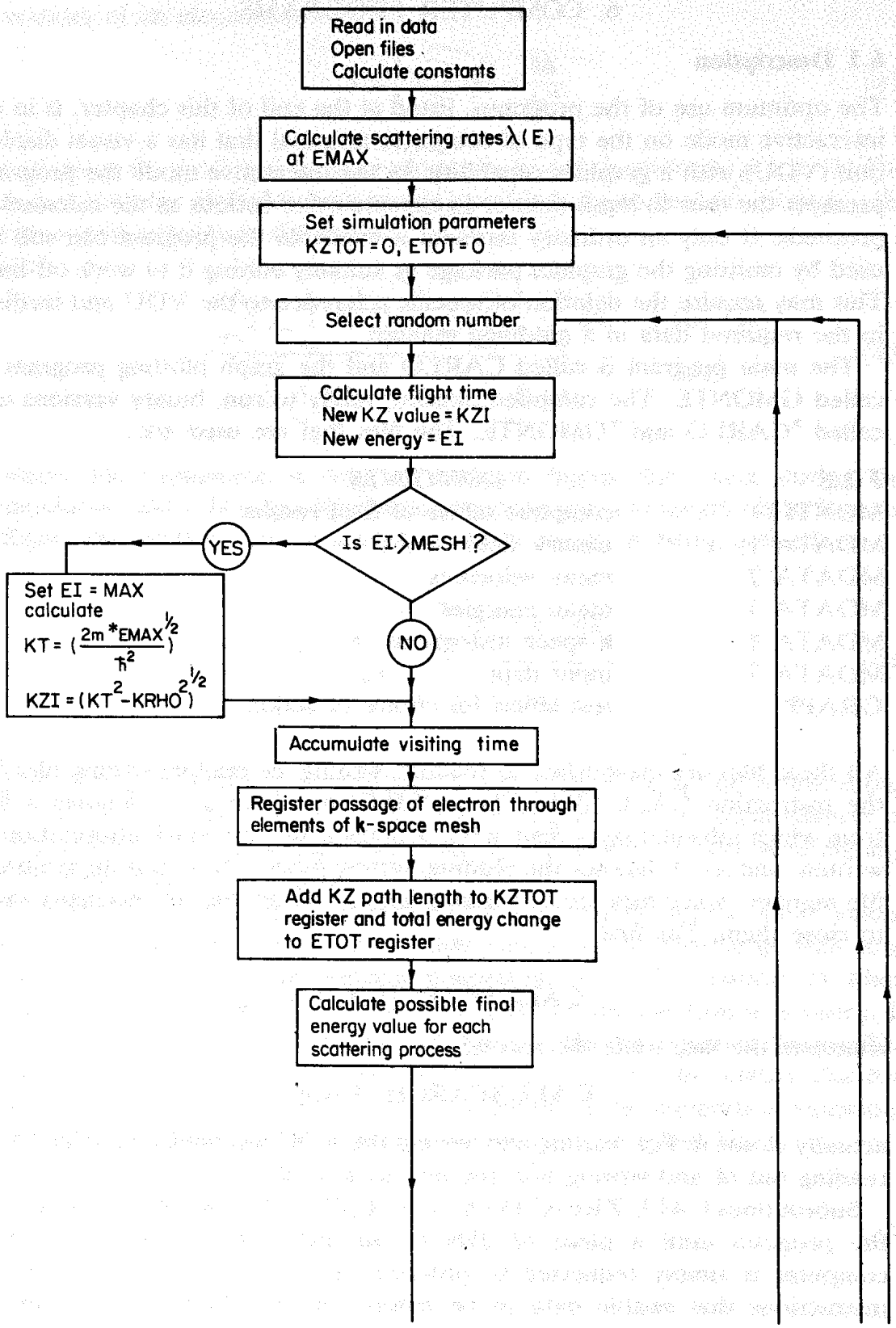
Read in data
Open files
Calculate constants
Calculate scattering rates λ(E) at EMAX
Set simulation parameters
KZTOT = 0, ETOT = 0
Select random number
Calculate flight time
New KZ value = KZI
New energy = EI
Is EI > MESH ?
YES
NO
Set EI = MAX
calculate
KT = (2m*EMAX/ħ²)^1/2
KZI = (KT² - KRHO²)^1/2
Accumulate visiting time
Register passage of electron through elements of k-space mesh
Add KZ path length to KZTOT register and total energy change to ETOT register
Calculate possible final energy value for each scattering process

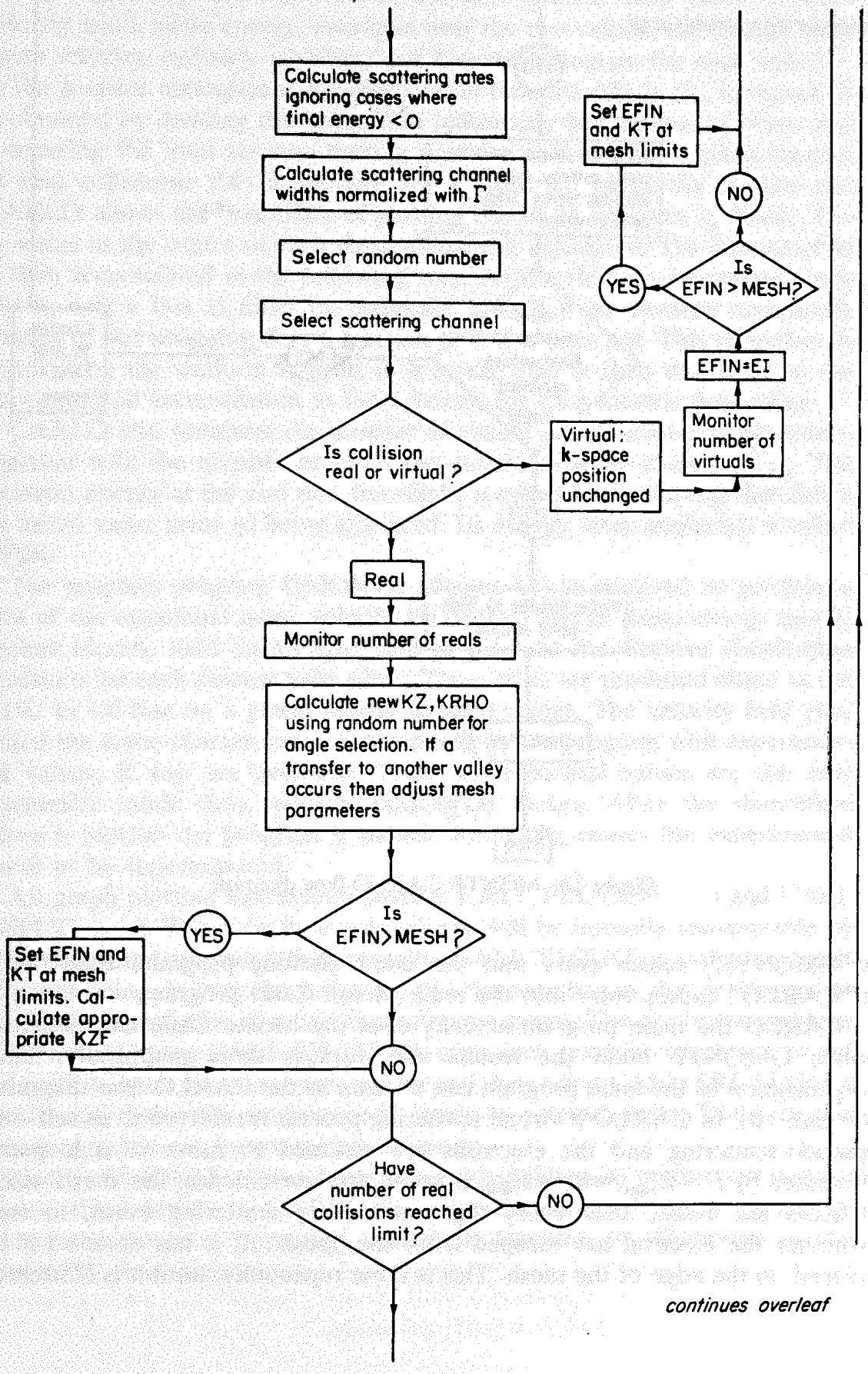

continues overleaf

continued from previous page

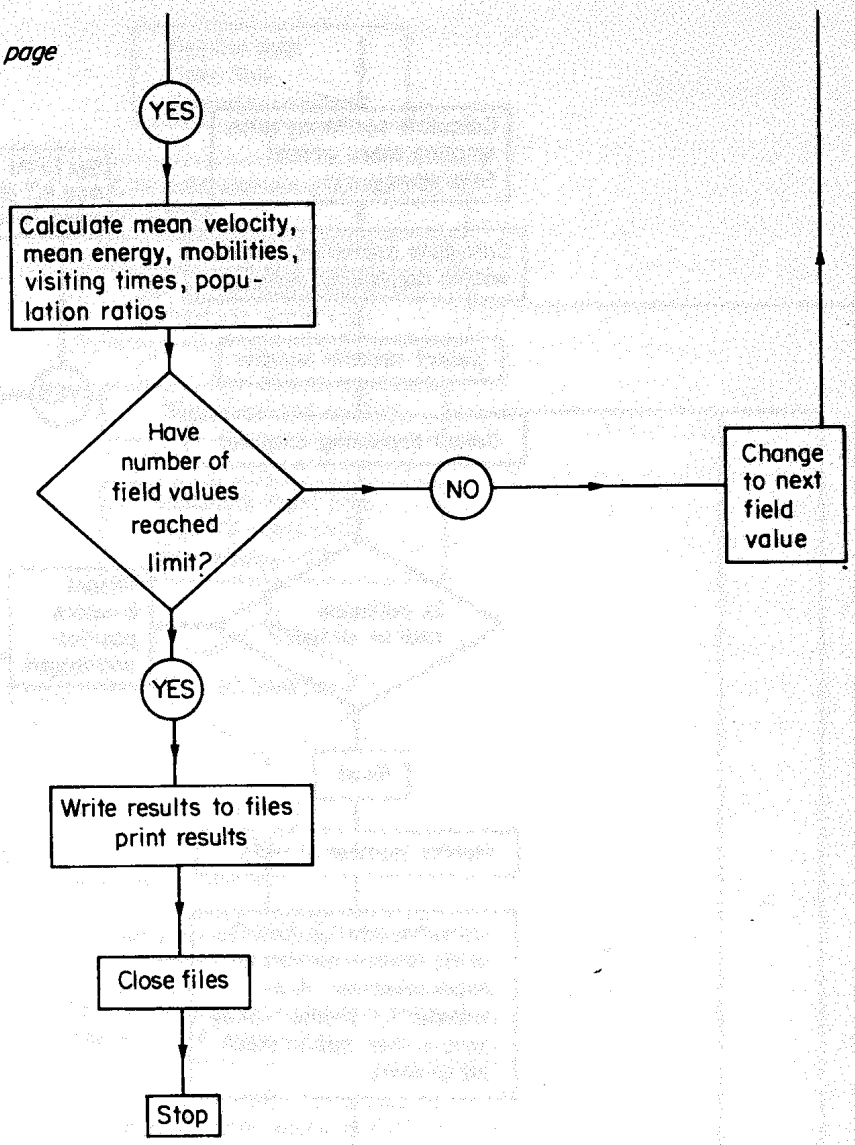

Figure 10. MONTE CARLO flow diagram

('*GMONTE') causes entry into the graph plotting program, RESUME ('*CARLO') causes entry into the main Monte Carlo program.

CARLO the main program actually does the Monte Carlo calculations, while GMONTE takes the results and displays them graphically. The organization of the main program can be seen in the CARLO flow diagram (Figure 10). In CARLO a virtual scattering process is referred to as self- or pseudo-scattering and the electrons are assumed to move in a **k**-space bounded by $E = E_{max}$, where E_{max} is called, for convenience, the 'mesh' size. Checks are made, after every flight and every scattering event, to see whether the electron has escaped from the 'mesh'. If it has done so it is placed on the edge of the mesh. This is done repeatedly, until it is scattered

inwards again. CARLO produces, for each electric field value, a mean velocity and a mean energy, averaged over the two valleys, the visiting time, mean velocity, ordinary mobility, and **k**-space histogram for each valley.

The **k**-space histogram is the distribution function $f(\mathbf{k})$ in (k_ρ, k_z) space. It is obtained by dividing this space into reasonably fine meshes or boxes and computing the total electron visiting time for each box for a given number of real collisions; $f(\mathbf{k})$ is plotted, for a fixed k_ρ. along the k_z-axis and CARLO allows the possibility of plotting this at 21 different k_ρ levels. The k_z-value at the centre of each mesh element is calculated. The function $f(\mathbf{k})$ is then accumulated in the following way. As the electron progresses along the k_z-axis a box is filled by assigning 1 to it if an electron completely crosses it, but assigning only a fraction to it if it does not. This procedure is justified by the uniform motion in **k**-space; $f(\mathbf{k})$ is then displayed as the unnormalized accumulation in these boxes, for each electric field value.

CARLO also monitors the number of virtual or self-scattering processes, together with the number of times the electron energy exceeds E_{max}. The electron energy at the end of a free-flight is called EI, indicating that this is its initial value prior to being scattered. Its energy after scattering is called EFIN.

The graphics program GMONTE (Figure 11) is designed to produce a plot of the calculated mean velocity (in cm/sec) and of mean energy (in eV) against electric field (in kV/cm), and to produce the electron distribution functions for each electric field value. These plots are produced either at the VDU or off-line on a graph plotter as hard copies. The velocity-field plot, called the static characteristic, is compared by the program with experimental values, if any are available. These experimental values are the only interactive mode data requests GMONTE makes. After the theoretical curve is plotted the program is halted. Restarting causes the experimental curve to be superimposed.

All graph plotting instructions involve CALL FIXAXS(. . . . .) and CALL FGPLT(. . . . .). These, or their equivalents, will be instantly recognizable by most computer program advisory units. CALL T1OU(7) is only an embellishment being, in fact, the activation of a warning buzzer that is sounded to signify the completion of a line of results or a graph. The display of graphs is held static by using CALL CHAMOD, after each graph is completed, to put the console back into a numeric mode, and then using CALL ZREALD(A). This simply halts the program until return is entered at the VDU. In this way the graphs can be examined at leisure.

Finally, GMONTE allows three other possibilities (a) production of hard copies, (b) a return to CARLO to rerun the Monte Carlo program, (c) ending the program operation. All these features are illustrated in the GMONTE flow diagram.

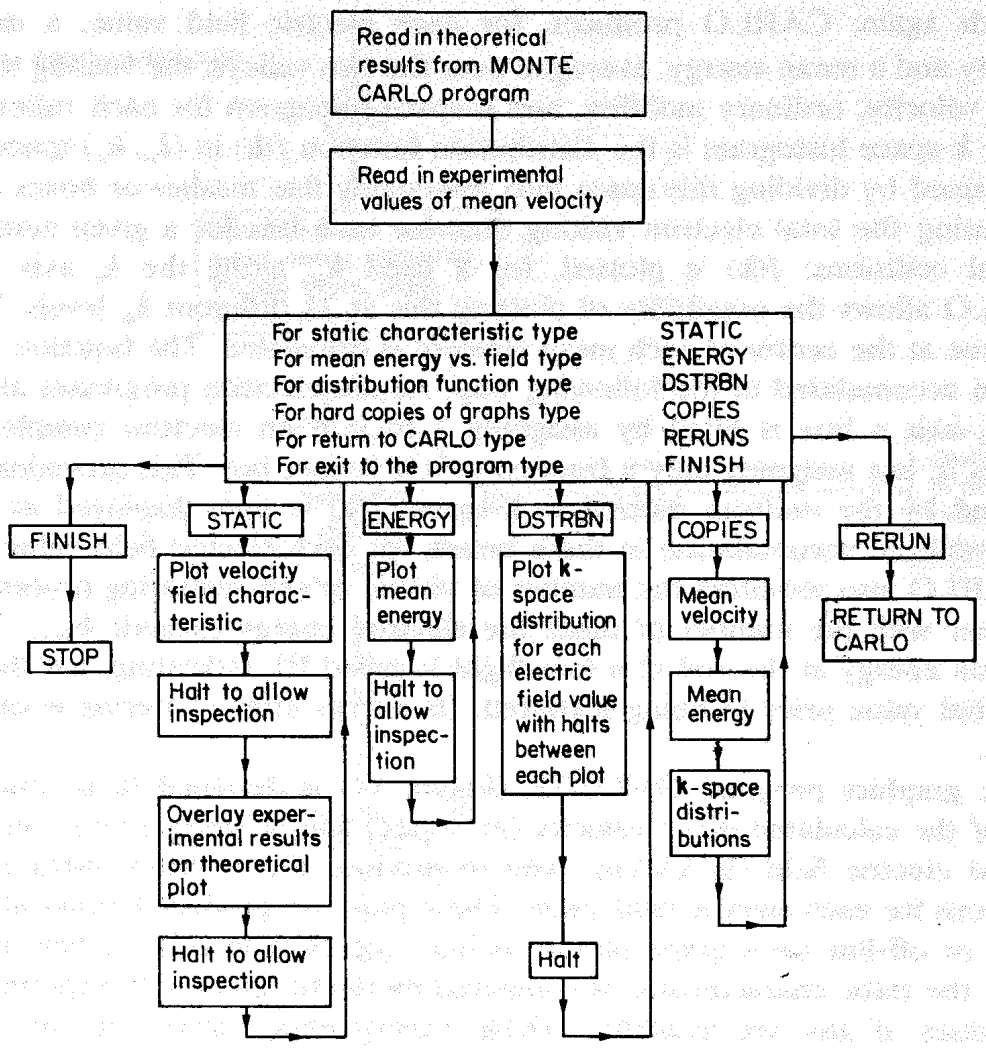

Figure 11. GMONTE flow diagram

6.2 Running the programs

The programs are quite straightforward to run since so many prompts are given to the user. The main program, CARLO, does not contain any graphics and can be run on any kind of terminal. The material data, specifying the semiconductor, are placed, for recall purposes, in the file MDATA5 and comprises, for GaAs, the values given in Table 2. On rerunning the program these data can be used again by typing OLD in response to the question FOR SAME MATERIAL DATA TYPE OLD, FOR NEW TYPE NEW.

An examination of the program listed soon reveals that most of the material parameters are fed in with scaled values since obvious powers of 10, and the free electron mass, are already built into it. Thus, for example, the deformation potential D_n is entered into the computer as 1.0. Furthermore, all energies are expressed in eV, wave numbers in cm^{-1}, and the scattering rates are calculated using cgs units.

The temperature of the solid, the maximum allowed energy and the maximum allowed number of real collisions are entered next. These quantities can be varied at will. However, for the example output, we have taken 300 K, 1 eV, and 2000. Such a temperature corresponds to room-temperature operation, but the temperature variation of the results should be investigated. An E_{max} of 1 eV is just about right, for this example, because we do not intend the electric field to exceed 10 kV/cm. Much higher fields may require a larger E_{max}. Also, too small a value would seriously, and artificially, distort the electron distribution causing the electron to be constantly leaving the 'mesh'. Too large a value would encourage occasional long flights that contribute very little towards the distribution function. Experimentation with E_{max} is, of course, a very interesting exercise. The program has a built-in limit to the number of real collisions (i.e. real scattering events) allowed. This can be changed quite easily. Indeed, it is only there to limit the time of a computer run. Obviously, accuracy is lost this way and the student would be well advised to run the program for a varying number of real collisions to check the rate of convergence. This is entertaining since a lot of good physics is learned through interpreting the shorter runs.

The next section of the data requests asks for the number of electric fields to be used, the values of these fields in units of kV cm^{-1}, and for which valley plots of the **k**-space distribution function are required. The number of electric fields used is a matter of choice; however, from the point of view of the time available, for experimentation a maximum number equal to seven is suggested. An initial trial run of the field values 1.0, 2.0, 3.0, 4.0, 5.0, 6.0, and 7.0 is recommended. Such a run will reveal, for GaAs, the negative differential mobility, with v against F having a peak near to 3.3 kV/cm. Then the peak area and any other region that looks interesting can be investigated more carefully.

After deciding to look at either the **k**-space distribution function of the central or satellite valley, a k_ρ level is selected. The population density, as measured by the content of the boxes, changes as each k_ρ is chosen and will fall off at very large k_ρ. Also, as a function of k_z, some form of rough Maxwellian distribution should be observed. If it is desired to simulate a simpler one-valley semiconductor then $\Delta = 0$ and the intervalley deformation potentials are set equal to zero.

For GaAs typical experimental values of mean velocity v cm/sec and electric field F kV/cm required by GMONTE are: (1.0, 0.85×10^7), (2.0, 1.63×10^7), (3.0, 2.15×10^7), (4.0, 2.00×10^7), (5.0, 1.80×10^7), (6.0, 1.60×10^7), (7.0, 1.45×10^7).

6.3 Output from the programs

After running CARLO the file MONTEF will contain some tables of final results and MDATA4 will contain the **k**-space histograms for the k_ρ level,

and for each value of electric field, requested. In addition MDATA1, MDATA2, and MDATA3 will contain, respectively, a table of electric field values, mean velocities, and mean energies. The contents of MONTEF, for the GaAs data discussed earlier, using the parameters suggested above, are listed at the end of the chapter under the heading Monte Carlo results. In this listing the following definitions are used.

FIELD : electric field value.
VELOCITY : mean electron velocity, in cm/sec, averaged over both valleys.
GAMMA1 : $\Gamma = \Gamma_1$ for central valley.
GAMMA2 : $\Gamma = \Gamma_2$ for satellite valleys.
TIME IN 1 : time in seconds spent central valley.
TIME IN 2 : time in seconds spent satellite valleys.
MN. ENERGY: mean electron energy in eV averaged over both valleys.
SELF : number of virtual collisions.
MESH : number of times electron energy exceeded E_{max}.
VEL1 : average velocity of electrons in central valley.
VEL2 : average velocity of electrons in satellite valleys.
MOB1 : mobility = VEL1/FIELD of electrons in central valley.
MOB2 : mobility = VEL2/FIELD of electrons in satellite valleys.
N1 : fraction of electron population in central valley.
N2 : fraction of electron population in satellite valleys.

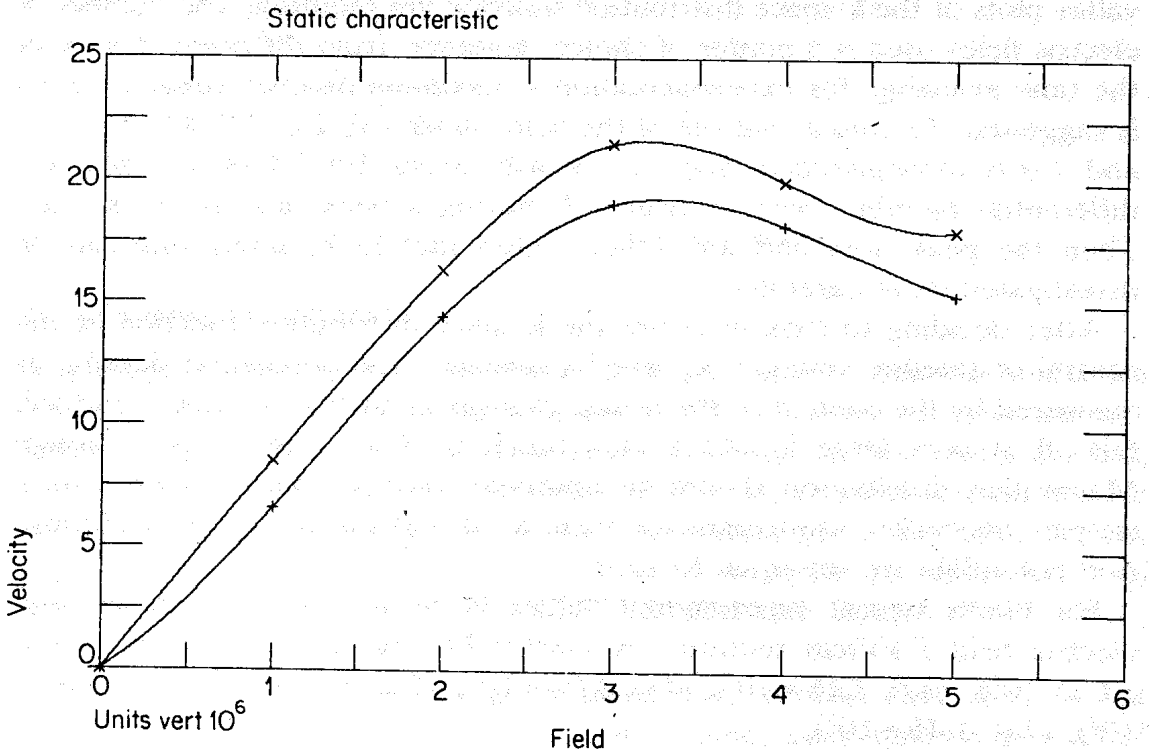

Figure 12. Computer-generated plot of mean velocity of electrons (cm/sec) as a function of applied electric field (kV/cm). + Monte Carlo simulation: 2000 real collisions; × experimental results

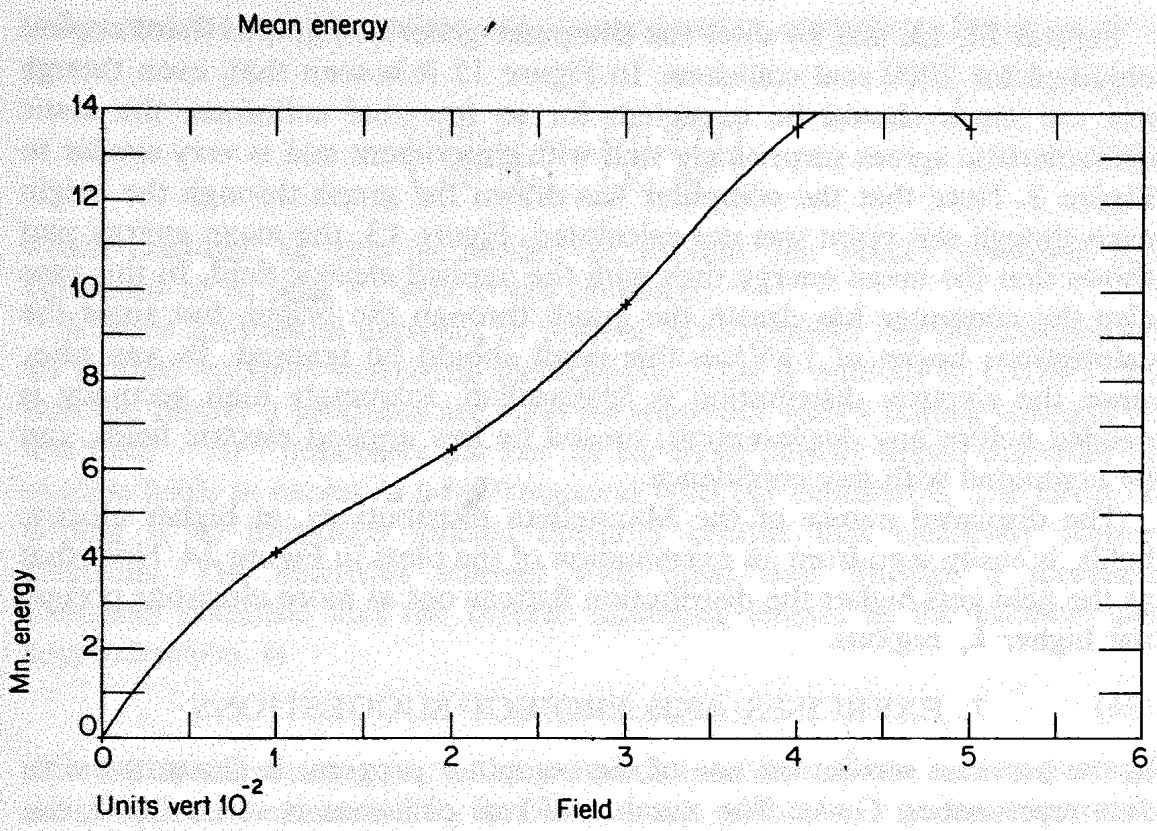

Figure 13. Computer-generated plot of electron mean energy (eV) as a function of applied electric field)kV/cm)

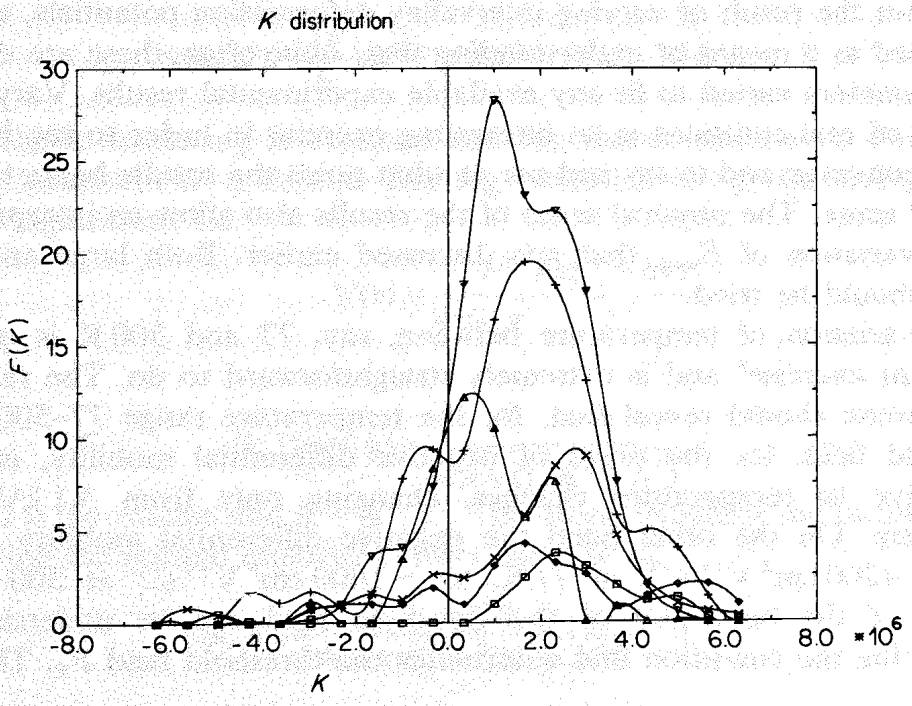

Figure 14. k-space distribution for different electric fields (F kV/cm). $\triangle$: $F=1$, ∇: $F=2$, $+$: $F=3$, $\times$: $F=4$, $\square$: $F=5$, $\diamond$: $F=6$

Figures 12, 13, and 14 show the computer-generated graphs (hard copies) obtained for 2000 real collisions. In Figure 12 it is seen that, even though not too much should be expected, for so few real collisions, the static characteristic agrees surprisingly well with experiment and is very similar to Figure 2. Note that the computer has drawn the graph through the origin even though this point was not calculated. Figure 13, the mean energy plot shows that the mean energy rises with the applied electric field. In this case also the computer has drawn the graph through the origin, but since the calculations began at 1 kV/cm this point should be ignored. In any case, since the electron distribution is Maxwellian, extremely high accuracy is needed before any displacement, caused by low applied electric fields, can be computed with any confidence.

The displaced nature of the Maxwellian distributions, at higher electric fields, is easily seen from an examination of the plots in Figure 14. Note that as the field gets higher the distribution flattens out as more electrons occupy the higher k_z regions.

7. EXERCISES AND PROJECT SUGGESTIONS

In the previous section the use of the computer program is illustrated with data representing GaAs. The number of real collisions is set at 2000, the maximum energy is set at 1 eV, and a temperature of 300 K is used. This set of data, however, leaves a lot of room for manoeuvre. Obviously, if GaAs is going to be studied then the material constants should not be altered too much, but the result of varying intervalley deformation potentials, say, can be studied as a means of understanding that, quite often, these are disposable parameters varied to fit any available experimental results. Varying the number of real collisions is an interesting exercise in order to see how the results converge and to try and see at what point the results begin to make physical sense. The physical sense of the results also allow an interpretation of the variation of E_{max} that was discussed earlier. Both large and small values should be tried.

The variation of temperature between, say, 77 and 500 K is quite an important exercise[9] and is extremely straightforward to do. The results of this exercise should reveal that, for the temperature range 77–500 K, the threshold field, for the onset of negative differential mobility, is rather insensitive to temperature changes, changing only from 3.1 kV/cm to 3.7 kV/cm. On the other hand the negative differential mobility reduces from $\sim 4200\,\mathrm{cm^2\,V^{-1}\,s^{-1}}$, at 77 K, to $\sim 1000\,\mathrm{cm^2\,V^{-1}\,s^{-1}}$ at 500 K. The physics of the behaviour of the threshold field can be understood by considering the condition that determines the threshold field F_T. This is

$$\left[\frac{\mathrm{d}}{\mathrm{d}F}(n_1 v_1)\right]_{F_{Th}} = 0, \tag{47}$$

where n_1 and v_1 are the electron concentration and velocity in the central

valley and the satellite valleys are assumed not to contribute. Equation (47) gives

$$\left[\left|\frac{dn_1}{dF}\right|\right]_{F_{Th}} = \left[\frac{n_1}{V_1}\frac{dV_1}{dF}\right]_{F_{Th}} \tag{48}$$

which contains all that is needed to explain the results provided the variations of n_1 and V_1 with F are obtained.

A more substantial exercise, or project, is to consider the introduction of an ionized impurity scattering mechanism.[9] This is omitted in CARLO so that the results it produces are valid for materials with a doping strength of less than $\sim 10^{15}$ impurities per cm^3 or for more heavily doped materials in electric fields in excess of a few thousand volts per centimetre. The effect of doping is to introduce ionized impurity centres that elastically scatter electrons. The electrons interact with these ions through a screened Coulomb potential and the inverse screening length, in the classical gas approximation, is

$$\Lambda^2 = ne^2/(4\pi\kappa_o k_B T\varepsilon), \tag{49}$$

where T is temperature, κ_0 is the permittivity of free space, ε is an average static dielectric constant, k_B is Boltzmann's constant, e is the electronic charge, and n is the electron density. Typically, even up to electron concentrations of 10^{17} cm^{-3}, Λ does not exceed $\sim 4\times 10^5$ cm^{-1}.

The transition probability, for ionized impurity scattering, is

$$S(\mathbf{k},\mathbf{k}') = \frac{2\pi}{\hbar}|\langle\mathbf{k}'|V(\mathbf{r})|\mathbf{k}\rangle|^2\delta(E(\mathbf{k}')-E(\mathbf{k})), \tag{50}$$

where elastic scattering is assumed and the matrix element is simply the Fourier transform of a Brooks–Herring potential energy (assuming singly ionized impurities), i.e.

$$V(r) = \frac{-e^2}{4\pi\kappa_0\varepsilon}\frac{\exp(-\Lambda r)}{r} \tag{51}$$

and

$$\langle\mathbf{k}'|V(\mathbf{r})|\mathbf{k}\rangle = \frac{-e^2}{\kappa_0\varepsilon\sqrt{\Omega}}\frac{1}{(K^2+\Lambda^2)}, \tag{52}$$

where Ω is the volume and $K = |\mathbf{k}-\mathbf{k}'|$. Therefore, including the factor $\Omega/8\pi^3$ and setting the ionized impurity density equal to n,

$$S(\mathbf{k},\mathbf{k}') = \frac{4e^4 n}{\hbar(4\pi\kappa_0)^2\varepsilon^2(K^2+\Lambda^2)^2} \tag{53}$$

and

$$\lambda(\mathbf{k}) = \frac{4\pi e^4 n 2\sqrt{2}m^{*\frac{1}{2}}E^{\frac{1}{2}}}{\hbar^2\varepsilon^2(r\pi\kappa_0)^2\Lambda^2[(\hbar^2\Lambda^2/2m^*)+4E]}. \tag{54}$$

It is only when $E > 0.005$ eV that the electron distribution function is not basically spherically symmetric.[9] This fact, together with the fact that $\Lambda \leqslant 4\times10^5\,\mathrm{cm}^{-1}$ for densities up to $10^{17}\,\mathrm{cm}^{-3}$, implies that $\hbar^2\Lambda^2/8mE \ll 1$. Hence,

$$\lambda(\mathbf{k}) \simeq \frac{\pi e^4 n 2\sqrt{2} m^{*\frac{1}{2}}}{\hbar^2 \varepsilon^2 (4\pi\kappa_0)^2 \Lambda^2 E^{\frac{1}{2}}} = \frac{2\sqrt{2}\pi e^2 m^{*\frac{1}{2}} k_B T}{\hbar^2 \varepsilon (4\pi\kappa_0) E^{\frac{1}{2}}} \tag{55}$$

It may appear to be a little strange that λ is not a function of n, but it should be remembered that this result is only approximately true. Furthermore, the important point is that the distribution of scattering angles is affected by the size of the electron density. The probability density of scattering an electron through angle θ is proportional to the scattering matrix element and to $\sin\theta$, i.e.

$$p(\theta) = \frac{A \sin\theta}{(2k^2(1-\cos\theta)+\Lambda^2)^2}, \tag{56}$$

where A is a constant. The application of the Monte Carlo principle[9] leads to

$$\cos\theta = 1 - \frac{2(1-r)}{1-r(4k^2/\Lambda^2)}, \tag{57}$$

where r is a uniformly distributed random number. The rest of the procedure is the same as it is for optical polar phonon scattering.

A word of warning is needed here because the ionized impurity scattering rate is an order of magnitude greater than the phonon rates. Scattering by phonons, however, has a much greater influence on the transport properties. Some inefficiency can be encouraged, therefore, if ionized impurity scattering is introduced without any de-weighting procedures. The straightforward method will work, of course, but the user should try to devise methods of self-consistently reducing λ and increasing θ.

Another interesting project would be to consider the combined effect of a constant magnetic field $\mathbf{B}$ and a constant electric field $\mathbf{F}$. The equation of motion in momentum space of an electron of charge e and crystal momentum $h\mathbf{k}$ is

$$\hbar\frac{\mathrm{d}\mathbf{k}}{\mathrm{d}t} = e\mathbf{F} + \frac{e\hbar}{m^*}\mathbf{k}\times\mathbf{B}. \tag{58}$$

For fields $\mathbf{F} = (F, 0, 0)$ and $\mathbf{B} = (0, 0, B)$. The solutions of this equation are[7]

$$k_x = \left(\frac{eE}{\omega\hbar} + k_y^{(0)}\right)\sin(\omega t) + k_x^{(0)}\cos(\omega t), \tag{59}$$

$$k_y = \left(\frac{eE}{\omega\hbar} + k_y^{(0)}\right)\cos(\omega t) - k_x^{(0)}\sin(\omega t) - \frac{eE}{\omega\hbar}, \tag{60}$$

where $(k_x^{(0)}, k_y^{(0)}$, and $k_z^{(0)})$ is the position of the electron at time $t=0$. These equations show that the electron rotates in a circular orbit in the k_x–k_y plane centred on the point $(0, -m^*E/\hbar B)$, with a frequency $\omega = eB/m^*$ (the cyclotron frequency) and radius $K=[k_x^{(0)2}+(k_y^{(0)}+m^*E/(\hbar B))^2]^{\frac{1}{2}}$.

Using the same accumulation ideas discussed earlier in this chapter, and measuring θ anticlockwise (in a coordinate system $k_x' = K\cos\theta$, $k_y' = K\sin\theta$) from some suitable reference line, say the k_x'-axis, summations over all flights gives[7]

$$v_y = \frac{\hbar}{m^*}\frac{\sum K(\cos\theta_1 - \cos\theta_2)}{\sum(\theta_2-\theta_1)} - \frac{E}{B} \tag{61}$$

$$v_x = \frac{\hbar}{m^*}\frac{\sum K(\sin\theta_2 - \sin\theta_1)}{\sum(\theta_2-\theta_1)} \tag{62}$$

where θ_1 is the initial angle and θ_2 is the final angle on any flight. These formulae arise because integrations over angular displacements are used now instead of over k_z as in equation (43), i.e. $\int_{\theta_1}^{\theta_2} \mathrm{d}\theta K\cos\theta$, etc. The mean electron energy is therefore

$$E = \frac{\hbar^2}{2m^*}\frac{\sum \int_{\theta_1}^{\theta_2}\left\{k_z^2 + k_x'^2 + \left(k_y' - \dfrac{eE}{\omega\hbar}\right)^2\right\}\mathrm{d}\theta}{\sum \int_{\theta_1}^{\theta_2}\mathrm{d}\theta}. \tag{63}$$

Therefore

$$\begin{aligned} \mathrm{E} &= \frac{\hbar^2}{2m^*}\frac{\sum \int_{\theta_1}^{\theta_2}\left\{k_z^2 + K^2 + \left(\dfrac{\mathrm{eE}}{\omega\hbar}\right)^2 - 2K\sin\theta\left(\dfrac{eE}{\omega\hbar}\right)\right\}\mathrm{d}\theta}{\sum(\theta_2-\theta_1)} \\ &= \frac{\hbar^2}{2m^*\sum(\theta_2-\theta_1)}\left\{\sum(k_z^2+K^2)(\theta_2-\theta_1) - \frac{2eE}{\omega\hbar}\sum K(\cos\theta_1-\cos\theta_2)\right\} + \tfrac{1}{2}m^*\left(\frac{E}{B}\right)^2. \end{aligned} \tag{64}$$

The mean value of a quantity A, averaged over two valleys and setting $S = \sum(\theta_2-\theta_1)$, is

$$\langle A\rangle = \frac{m_1 S_1\langle A\rangle_1 + m_2 S_2\langle A\rangle_2}{m_1 S_1 + m_2 S_2}. \tag{65}$$

The determination of the distribution of scattering angles is more difficult than in the zero magnetic field case. A scattering event taking the electron

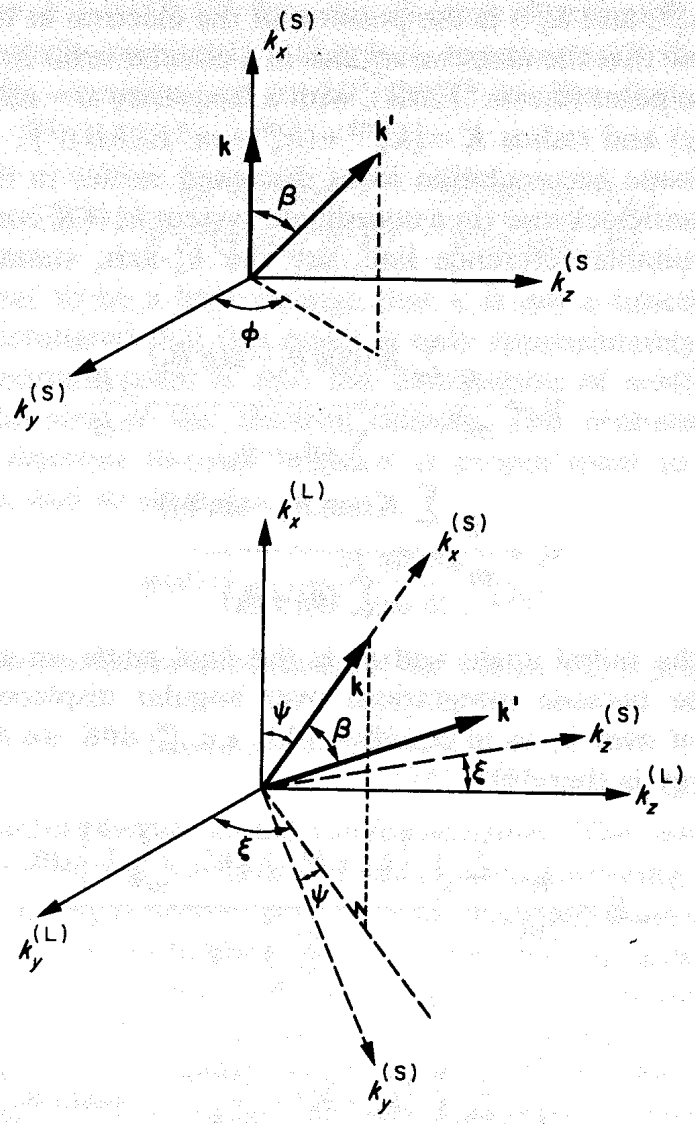

Figure 15. Scattering geometry of an electron in crossed electric and magnetic fields

from $\mathbf{k}$ to $\mathbf{k}'$ is shown in Figure 15. The components of $\mathbf{k}'$ are, in what we will call the scattering frame,

$$\begin{aligned} k_x^{(S)} &= k' \cos\beta, \\ k_y^{(S)} &= k' \sin\beta \cos\phi, \\ k_z^{(S)} &= k' \sin\beta \cos\phi. \end{aligned} \tag{66}$$

If a laboratory frame is now defined then, as ia really seen from Figure 15, the vector $\mathbf{k}^{(L)}$ is related to $k^{(S)}$ through

$$\begin{pmatrix} k_x^{(L)} \\ k_y^{(L)} \\ k_z^{(L)} \end{pmatrix} = \begin{pmatrix} \cos\psi & -\sin\psi & 0 \\ \sin\psi\cos\xi & \cos\psi\cos\xi & -\sin\xi \\ \sin\psi\sin\xi & \cos\psi\sin\xi & \cos\xi \end{pmatrix} \begin{pmatrix} k_x^{(S)} \\ k_y^{(S)} \\ k_z^{(S)} \end{pmatrix}, \tag{67}$$

where $k_x^{(L)}$, $k_y^{(L)}$, and $k_z^{(L)}$ are the **k**-space coordinates of the electron after a scattering event and $k' = \sqrt{2mE'}/\hbar$; $E' = E_f \pm \hbar\omega$, where E_f is the electron energy at the end of a flight.

The angle β is found in the usual way and the angles ξ, ψ are found as follows. At the end of a flight, and before a scattering event occurs,

$$\begin{aligned} k_x^{(f)} &= k \cos\psi. \\ k_y^{(f)} &= k \sin\psi \cos\xi, \\ k_z^{(f)} &= k \sin\psi \sin\xi \end{aligned} \tag{68}$$

so that

$$\cos\psi = \frac{k_x^{(f)}}{k}, \qquad \sin\xi = \frac{k_z^{(f)}}{\sqrt{k_x^{(f)2} + k_z^{(f)2}}}, \tag{69}$$

ϕ is a random angle and is part of the polar scattering. It is therefore determined in the same way, i.e. $\phi = 2\pi r$.

Acoustic and intervalley scattering must also be treated in three dimensions, but the results are quite straightforward. If the polar coordinates of an electron in **k**-space, after scattering, are θ, ϕ then $\cos\theta = 1 - 2r_1$, $\phi = 2\pi r_2$, where r_1 and r_2 are two random uniformly distributed numbers.

The student with all this information should now be in a position to modify the computer program given here and make a study of magnetic field effects, bearing in mind that the **k**-space histogram is no longer relevant since the system now has cylindrical symmetry. Many interesting quantities can be obtained, but perhaps the most interesting is that a complete

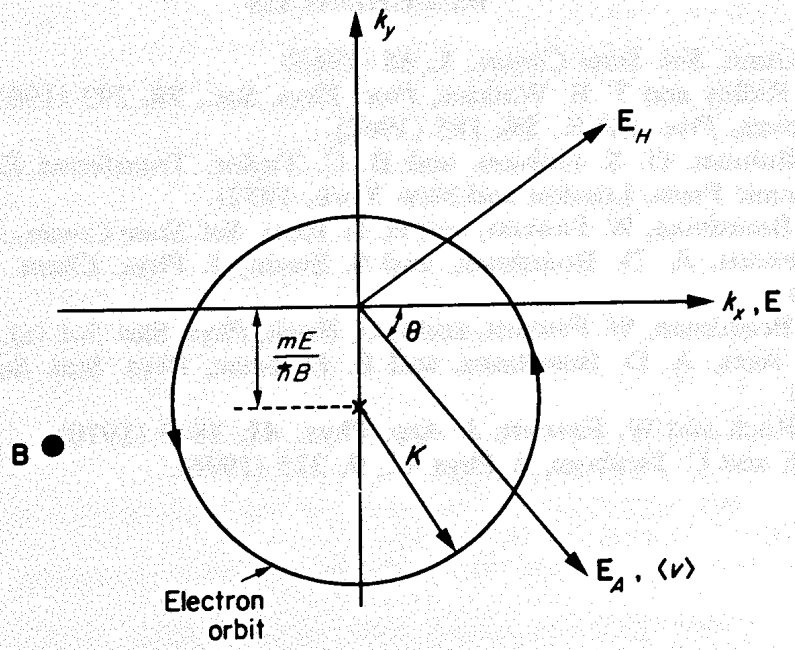

Figure 16. Schematic representation of the electron trajectory in k-space under the influence of crossed electric (E) and magnetic fields (B)

simulation of the Hall effect is possible. In Figure 16 it is seen that $E \cos \theta$ is interpreted as the applied field E_A and $E \sin \theta$ as the Hall field E_H. The Hall coefficient R_H is also given directly, the general definition of which is

$$R_H = \frac{E_H}{BJ}, \tag{70}$$

where J is the current density given by nev, n being the electron concentration. R_H is related to a scattering factor r through

$$R_H = \frac{r}{ne}, \tag{71}$$

so that

$$r = \frac{E_H}{Bv} = \frac{\mu_H(B)}{\mu_D(B)}, \tag{72}$$

where $\mu_D(B) = v/E_A$ is the drift mobility and $\mu_H(B) = E_H/BE_A$ is the Hall mobility.

These are some of the short-term and long-term exercises, and projects, that can be attempted. Obviously there are many others, such as the inclusion of non-parabolity[6] and accounting for the Pauli exclusion principle as the electron gas becomes degenerate.[10] These are not discussed here but the answers can be found by studying the references at the end of the chapter.

REFERENCES

1. J. B. Gunn, *Sol. State Comm.*, **1,** 88 (1963).
2. B. K. Ridley and T. B. Watkins, *Proc. Phys. Soc.*, **78,** 293 (1961).
3. C. Hilsum, *Proc. I.R.E.*, **50,** 185 (1962).
4. P. J. Bulman, G. S. Hobson, and B. C. Taylor, *Transferred Electron Devices* (Academic Press, London and New York, 1972).
5. A. D. Boardman, W. Fawcett, and H. D. Rees, *Sol. State Comm.*, **6,** 305 (1968).
6. W. Fawcett, A. D. Boardman, and S. Swain, *J. Phys. Chem. Sol.*, **31,** 1963 (1970).
7. A. D. Boardman, W. Fawcett, and J. G. Ruch, *Phys. Stat. Sol.* (a), **4,** 133 (1971).
8. G. C. Aers, A. D. Boardman, and E. D. Isaac, *Phys. Stat. Sol.* (a), **36,** 357 (1976).
9. J. G. Ruch and W. Fawcett, *J. App. Phys.*, **41,** 3843 (1970).
10. S. Bosi and C. Jacaboni, *J. Phys. C.*, **9,** 315 (1976).

MONTE CARLO RESULTS

GAMMA1= 0.7212E 14 GAMMA2= 0.7921E 14
TEMP=0.3000E 03 REALCOLSNS= 2000 MAXENERGY(EV)=1.00

FIELD	VELOCITY	TIME IN 1	TIME IN 2	MN.ENERGY	SELF	MESH
0.100E 01	0.659E 07	0.458E-09	0.000E 00	0.413E-01	30663	0
0.200E 01	0.144E 08	0.371E-09	0.864E-11	0.644E-01	25469	0
0.300E 01	0.190E 08	0.272E-09	0.242E-10	0.972E-01	19376	0
0.400E 01	0.182E 08	0.149E-09	0.502E-10	0.137E 00	12706	0
0.500E 01	0.154E 08	0.862E-10	0.615E-10	0.137E 00	8983	0
0.600E 01	0.122E 08	0.651E-10	0.679E-10	0.125E 00	8065	0

FIELD	VEL1	VEL2	MOB1	MOB2	N1	N2
0.100E 01	0.659E 07	0.000E 00	0.659E 04	0.000E 00	0.100E 01	0.615E-01
0.200E 01	0.147E 08	0.269E 07	0.734E 04	0.135E 04	0.977E 00	0.227E-01
0.300E 01	0.207E 08	0.116E 0	0.691E 04	0.385E 0	0.918E 00	0.817E-01
0.400E 01	0.240E 08	0.107E 07	0.600E 04	0.268E 03	0.748E 00	0.252E 00
0.500E 01	0.250E 08	0.194E 07	0.500E 04	0.388E 03	0.584E 00	0.416E 00
0.600E 01	0.236E 08	0.128E 07	0.394E 04	0.214E 03	0.490E 00	0.510E 00